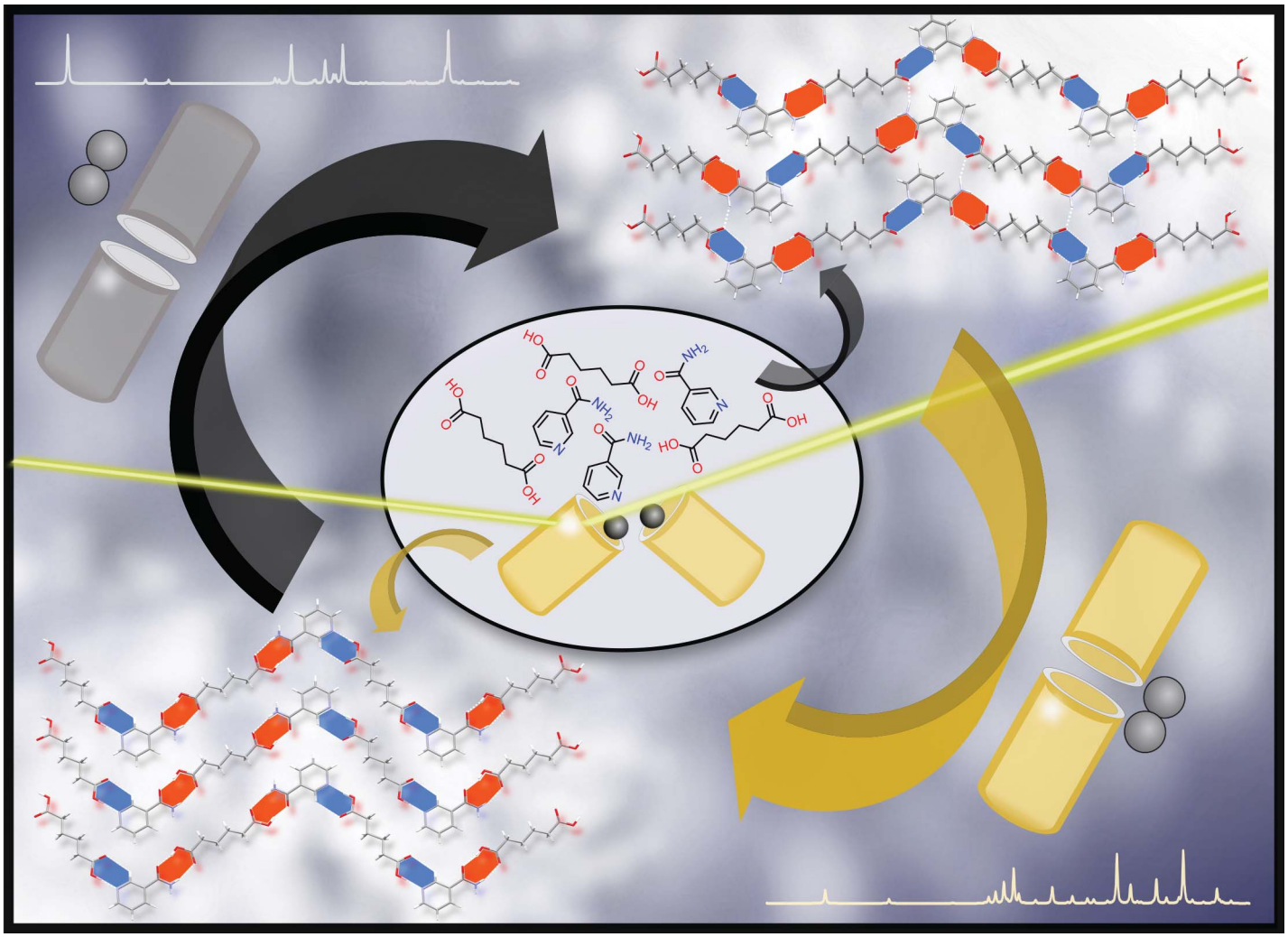

Showcasing research from Professor Friščić's laboratory, Department of Chemistry, McGill University, Canada and Professor Dinnebier's laboratory, Max Planck Institute for Solid State Research, Stuttgart, Germany.

Challenging the Ostwald rule of stages in mechanochemical cocrystallisation

We present a hitherto unexplored mechanochemistry-based route for controlling polymorphism of organic solids, simply by using different choices of the milling assembly (*i.e.* milling balls and jars) material to direct the polymorphic outcome of mechanochemical cocrystallisation. Changes to the choice of milling media (*i.e.* number and material of milling balls) and/or milling vessel material have been used to direct the appearance of cocrystal polymorphs in mechanochemical cocrystallisation along or against Ostwald's rule of stages, while enabling the selective synthesis, and even reversible interconversion of polymorphs.

As featured in:

See Luzia S. Germann, Tomislav Friščić *et al.*, *Chem. Sci.*, 2020, **11**, 10092.

ROYAL SOCIETY OF CHEMISTRY

rsc.li/chemical-science

Registered charity number: 207890

Chemical Science

ROYAL SOCIETY OF CHEMISTRY

EDGE ARTICLE

View Article Online
View Journal | View Issue

Cite this: *Chem. Sci.*, 2020, **11**, 10092

All publication charges for this article have been paid for by the Royal Society of Chemistry

Challenging the Ostwald rule of stages in mechanochemical cocrystallisation†‡

Luzia S. Germann, *[ab] Mihails Arhangelskis, [bc] Martin Etter, [d] Robert E. Dinnebier [a] and Tomislav Friščić *[b]

Mechanochemistry provides an efficient, but still poorly understood route to synthesize and screen for polymorphs of organic solids. We present a hitherto unexplored effect of the milling assembly on the polymorphic outcome of mechanochemical cocrystallisation, tentatively related to the efficiency of mechanical energy transfer to the milled sample. Previous work on mechanochemical cocrystallisation has established that introducing liquid or polymer additives to milling systems can be used to direct polymorphic behavior, leading to extensive studies how the amount and nature of grinding additive affect reaction outcome and polymorphism. Here, focusing on a model pharmaceutical cocrystal of nicotinamide and adipic acid, we demonstrate that changes to the choice of milling media (*i.e.* number and material of milling balls) and/or the choice of milling assembly (*i.e.* jar material) can be used to direct polymorphism of mechanochemical cocrystallisation, enabling the selective synthesis, and even reversible and repeatable interconversion of cocrystal polymorphs. While real-time mechanistic studies of mechanochemical transformations of metal–organic materials have previously suggested that reactions follow a path described by Ostwald's rule of stages, *i.e.* from metastable to increasingly more stable product structures, the herein presented systematic study presents an exception to that rule, revealing that modification of energy input in the mechanochemical system, combined with a small energy difference between polymorphs, permits the selective synthesis of either the more stable room temperature form, or the new metastable high-temperature form, of the target cocrystal.

Received 1st July 2020
Accepted 29th July 2020

DOI: 10.1039/d0sc03629c

rsc.li/chemical-science

Introduction

Mechanochemistry, *i.e.* the application of mechanical agitation as a way to conduct chemical transformations, is rapidly emerging as a cornerstone of greener, sustainable solvent-free strategies for molecular and materials synthesis,[1,2] ranging from covalent[3,4] and metal–organic frameworks (COFs and MOFs, respectively),[5] coordination polymers,[6] nanoparticle systems,[7] to molecular cages,[8] small molecules,[9,10] and cocrystals.[11,12] It has been shown that mechanochemistry is not only efficient for the synthesis of new metastable solid phases, but also a superior technique for polymorph and cocrystal screening, enabling the discovery of previously not observed thermodynamically stable phases even in well-studied systems.[13]

Mechanochemical reactions are often performed by direct grinding or milling of reactants alone (neat grinding), or in presence of additives, as in liquid-assisted grinding (LAG)[14] or polymer-assisted grinding (POLAG).[15] The choice[16–19] or amount of liquid additive[16] in LAG, measured through the η-parameter[14] (liquid-to-solid ratio in μL mg^{-1}), can strongly influence mechanochemical reactions, and has been shown to enable modification of mechanochemical reaction mechanism,[20] leading to different intermediates,[21] or diverse product polymorphs.[16–19,22] However, the factors that direct product formation in mechanochemistry remain poorly understood. Monitoring the progress of mechanochemical transformations *in situ* and *ex situ* has given evidence for complex reaction mechanisms, with multiple crystalline phases appearing as intermediates *en route* to the final product.[5a,20,21] At least in the context of MOF formation,[23a,b] theoretical and experimental studies have indicated that such reaction sequences can be explained by Ostwald's rule of stages, *i.e.* relaxation of a system from a high energy state into the thermodynamically stable form *via* a series of increasingly stable intermediates.[23c] Whereas such thermodynamic considerations may suggest

[a]*Max Planck Institute for Solid State Research, Heisenbergstr. 1, 70569 Stuttgart, Germany*

[b]*Department of Chemistry, McGill University, 801 Sherbrooke St. W., H3A 0B8 Montreal, Canada. E-mail: luzia.germann@mail.mcgill.ca; tomislav.friscic@mcgill.ca*

[c]*Faculty of Chemistry, University of Warsaw, 1 Pasteura Street, 02-109 Warsaw, Poland*

[d]*Deutsches Elektronen Synchrotron (DESY), Notkestraße 85, 22607 Hamburg, Germany*

† This work is dedicated to Prof. Joel Bernstein (1941–2019).

‡ Electronic supplementary information (ESI) available. CCDC 1981453. For ESI and crystallographic data in CIF or other electronic format see DOI: 10.1039/d0sc03629c

a route to predict the course of mechanochemical reactions,[12b,23d] it remains unclear whether mechanochemical reactions of organic and metal–organic materials generally conform to Ostwald's rule of stages. While it is well established that milling frequency,[24–26] reaction jar filling,[26,27a,28] size or mass of milling media[26,27b,30–32] all affect rates of product formation, there are only a handful of reports discussing the influence of energy input,[26,27,31,33,34] mixing properties, or design of the milling assembly in organic mechanochemistry.[26,31,34–37] In fact, the latter appears to have remained unexplored in the context of polymorphism in mechanochemical reactions.[37]

Here, we demonstrate a hitherto unexplored effect of the milling assembly, specifically the choice and material of milling jar and balls, on the polymorphism in mechanochemical cocrystallization (Fig. 1). This effect has resulted in the discovery of a previously not known metastable polymorph of a known model pharmaceutical cocrystal simply by changing the kind of milling balls or jar material. Moreover, changing the jar material enabled the reliable and repeatable interconversion between two cocrystal polymorphs simply by using different jar materials, *e.g.* stainless steel (**ss**) *vs.* poly(methyl methacrylate) (PMMA). While prior work suggested that mechanochemical reactions are likely to follow Ostwald's rule of phases, the herein presented reversible mechanochemical polymorph conversion contrasts such studies, and shows that different choices of the milling assembly can permit the selective formation of either thermodynamically more stable or metastable polymorphs of an organic cocrystal, independent of any external liquid or polymer additives.

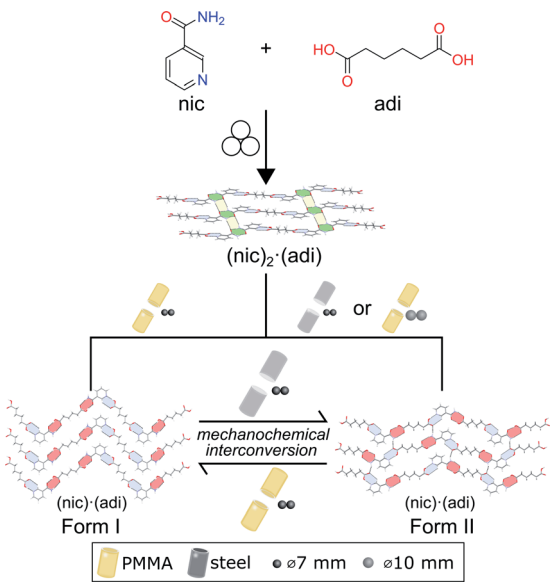

Fig. 1 Schematic representation of the herein presented work, revealing that mechanochemical cocrystallisation of **nic** and **adi** can produce different, enantiotropically-related polymorphs Form I and Form II of the cocrystal (**nic**)·(**adi**), depending on the choice of the milling assembly. Similarly, milling the pre-made cocrystal polymorphs in either a PMMA or a **ss** milling jar enables the selective formation of either thermodynamicaly more stable Form I, or the metastable Form II, respectively. Sign for mechanochemistry (three balls) adapted from Rightmire and Hanusa.[29]

Results and discussion

Mechanochemical discovery of new polymorph

As the model system we used cocrystallisation of the active pharmaceutical ingredient (API) nicotinamide (**nic**) with the cocrystal former (coformer) adipic acid (**adi**). While the two are known to form cocrystals of 1 : 1 and 2 : 1 respective stoichiometries,[38] this work also led to the discovery and characterisation of a new, metastable (**nic**)·(**adi**) cocrystal polymorph (see section on evaluation of polymorph stability). Milling of **nic** and **adi** in a 1 : 1 molar ratio in the presence of acetonitrile (ACN) as liquid additive ($\eta = 0.125$ μL mg^{-1}) and two stainless steel (**ss**) balls of 7 mm diameter (1.4 g each) in PMMA jars led to the

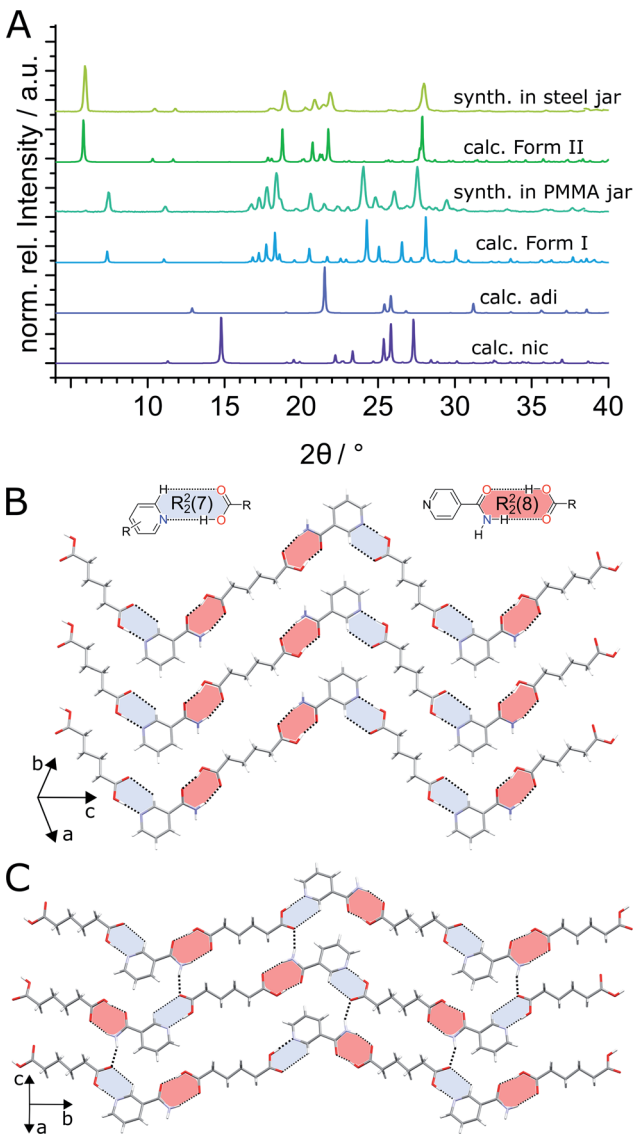

Fig. 2 (A) Comparison of measured and calculated XRPD patterns for mechanochemical synthesis of the (**nic**)·(**adi**) cocrystal by LAG with ACN (from top to bottom): in a **ss** jar, calculated Form II, in a PMMA jar, calculated for Form I (CSD code NUKYIC), calculated for **adi** (CSD code ADIPAC04) and calculated for **nic** (CSD code NICOAM03). Fragments of the crystal structures for: (B) previously reported Form I (**nic**)·(**adi**) (CSD NUKYIC) and (C) herein reported Form II (**nic**)·(**adi**).

formation of the previously known **(nic)·(adi)** cocrystal (CSD code NUKYIC), herein termed Form I (Fig. 2A and B). Comparison of measured and calculated X-ray powder diffraction (XRPD) patterns indicated that reaction was complete, with Form I **(nic)·(adi)** being the only crystalline phase in the reaction mixture, after *ca.* 60–90 min of milling (Fig. 2B). Surprisingly, repeating the reaction in **ss** jars under otherwise identical conditions led to the formation of a different material – a hitherto unknown **(nic)·(adi)** polymorph,‡ herein designated as Form II (Fig. 2A). Form II was found to be the enantiotropically related high-temperature phase of the thermodynamically more stable Form I (see section "Experimental and theoretical evaluation of polymorph stability"). The crystal structure of Form II was established from a combined XRPD and solid-state nuclear magnetic resonance (ssNMR) spectroscopy analysis (Fig. 2C, S1, S2B and S14–S18 in ESI‡). Both polymorphs consist of hydrogen-bonded zig-zag chains of alternating **nic** and **adi** molecules, connected by $R_2^2(7)$ pyridine-acid and $R_2^2(8)$ amide-acid heterosynthons (Fig. 2B and S2‡). Importantly, **adi** molecules in Form I lie on a centre of inversion, with each molecule involved in either two $R_2^2(7)$ or two $R_2^2(8)$ synthons (Fig. 2B). In contrast, each molecule of **adi** in Form II is involved in both a $R_2^2(7)$ and a $R_2^2(8)$ motif (Fig. 2B, C and S2‡).

In order to verify whether the observed difference in polymorphic outcome of the reaction is indeed associated with the choice of milling jar material, we compared products of milling **nic** and **adi** either neat, or by LAG in the presence of different liquid additives (H_2O, MeOH, $MeNO_2$, at a constant η value of 0.125 μL mg^{-1}), in either PMMA or **ss** jars. All explored LAG reactions produced a different outcome depending whether the reactions were conducted in **ss** or PMMA jars (Fig. S3‡). While the thermodynamically more stable Form I was preferably formed in PMMA jars, reactions in **ss** jars tended to produce the metastable Form II. This confirms a profound effect of the milling jar material on the reaction outcome, regardless of the choice of milling additive.

Reactions by neat grinding in either **ss** or PMMA jars, as well as LAG with water in a **ss** jar, were found to be slower and incomplete,§ producing mixtures of Forms I and II or **(nic)·(adi)** with or without the stoichiometrically different **(nic)$_2$·(adi)** cocrystal (CSD code NUKYOI). The **(nic)$_2$·(adi)** cocrystal was subsequently identified as the first reaction intermediate by *in situ* monitoring (see *In situ* X-ray powder diffraction section).

While previous studies of LAG cocrystallisation have focused on the choice and/or amount of liquid additive as the principal factor controlling product polymorphism, these experiments clearly show a strong effect of the composition of the milling assembly on polymorphism in cocrystallisation.

Mechanochemical polymorph interconversion

The evident influence of jar material on mechanochemical cocrystallisation can be used to control the polymorphic form of the resulting cocrystal through post-synthetic interconversion (Fig. 3A). This was evidenced by milling a sample of mechanochemically prepared Form I in a **ss** jar, using a pair of **ss** balls (7 mm diameter each) in the presence of ACN ($\eta = 0.125$ μL mg^{-1}).

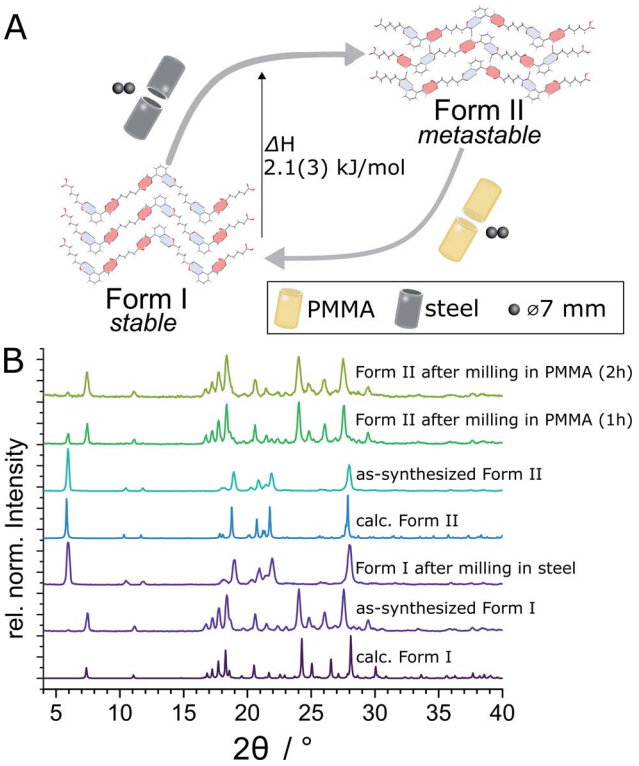

Fig. 3 (A) Schematic illustration of the herein demonstrated post synthetic interconversion of **(nic)·(adi)** polymorphs by milling in either PMMA or **ss** jar. The transition enthalpy ($\Delta H = +2.1(3)$ kJ mol^{-1} at the transition temperature) for the metastable Form II with respect to Form I was determined by DSC. (B) Comparison of XRPD patterns for post-synthetic interconversion of **(nic)·(adi)** Forms I and II (top-to-bottom): Form II after 2 hours milling in a PMMA jar; Form II after 1 hour milling in a PMMA jar; as-prepared Form II; calculated XRPD pattern of Form II; Form I after 1 hour milling in a **ss** jar; as-prepared Form I; calculated XRPD pattern of Form I (CSD NUKYIC).

Milling produced phase-pure Form II within 60 minutes. Conversely, Form II prepared by this mechanochemical process was found to transform into Form I upon milling in a PMMA jar under otherwise identical conditions. The conversion of Form II into Form I was slower than the opposite process, as evidenced by a weak diffraction signal corresponding to small amounts of residual Form II after 2 hours milling (Fig. 3B). To the best of our knowledge, the described results represent the first demonstration of reversible mechanochemical polymorph interconversion between stable and metastable phases, achieved simply by modification of the milling assembly.

In situ X-ray powder diffraction

We further explored mechanochemical cocrystallisation of **nic** and **adi** by monitoring the reaction through *in situ* synchrotron XRPD. Reaction monitoring was performed at the Powder Diffraction and Total Scattering beamline P02.1 of the Deutsches Elektronen-Synchrotron (DESY). All experiments were conducted using an in-house modified Retsch MM400 mill operating at 30 Hz,[39] in 15 mL volume PMMA jars, with ACN as the liquid additive ($\eta = 0.125$ μL mg^{-1}). X-ray transparent

PMMA jars were used exclusively in order to minimise intrinsic X-ray absorption and scattering arising from the milling jars. Milling experiments were performed using either two (experiment A) or four (experiment B) **ss** balls of 7 mm diameter (1.4 g each), or two zirconia (ZrO_2) balls of 10 mm diameter (2.9 g each, experiment C), leading to a total ball weight of 2.8, 5.6, and 5.8 g, respectively. In all cases, *in situ* observation revealed an initial formation of **(nic)$_2$·(adi)** as the (first) reaction intermediate (Fig. 4 and 5A).

In experiment A, milling with two **ss** balls led to gradual conversion of **(nic)$_2$·(adi)** into the known Form I **(nic)·(adi)** as the final product, with the reaction reaching completion after *ca.* 85 minutes milling (Fig. 4A). Next, we monitored the mechanochemical cocrystallisation using four **ss** balls of 1.4 g weight each (total balls weight 5.6 g), effectively doubling the total ball mass. Increasing the weight of milling media in experiment B corresponds to an increase in energy delivered to the reaction system, and is anticipated to lead to an increase in reaction rate.[32] Such an increase was indeed observed, along with the transient appearance of Form II of the **(nic)·(adi)** cocrystal. Forms I and II appeared concomitantly and their content increased almost simultaneously, indicating the conversion of the intermediate **(nic)$_2$·(adi)** *via* two competing pathways. However, the content of Form II reaches a maximum after *ca.* 15 minutes milling and is depleted soon after, while the amount of Form I steadily increases. This can be explained by most of the reaction mixture being converted to a mixture of Forms I and II after *ca.* 15 minutes, making apparent the process of mechanochemical conversion of Form II into Form I, which remains the final product after reaching a steady-state within *ca.* 40 min (Fig. 4B). Overall, *in situ* monitoring of experiment B reveals that milling under harsher reaction conditions, accomplished by increasing the overall weight of milling media from 2.8 g to 5.6 g, enabled the observation of a metastable intermediate. Such behavior is consistent with Ostwald's rule of stages that anticipates the appearance of metastable, high-energy intermediate phases, as the system is developing towards the thermodynamically preferred phase.

In experiment C (Fig. 4C), the reaction was repeated under identical conditions, but using two 10 mm ZrO_2 balls (2.9 grams each), of approximately the same weight (total of 5.8 grams) as the four **ss** balls used in experiment B. This enabled conducting a mechanochemical reaction in which the energy being brought to the milling assembly is nearly identical to that in experiment B, but distributed in a different way. This led to a further acceleration of the first reaction step with the initial formation

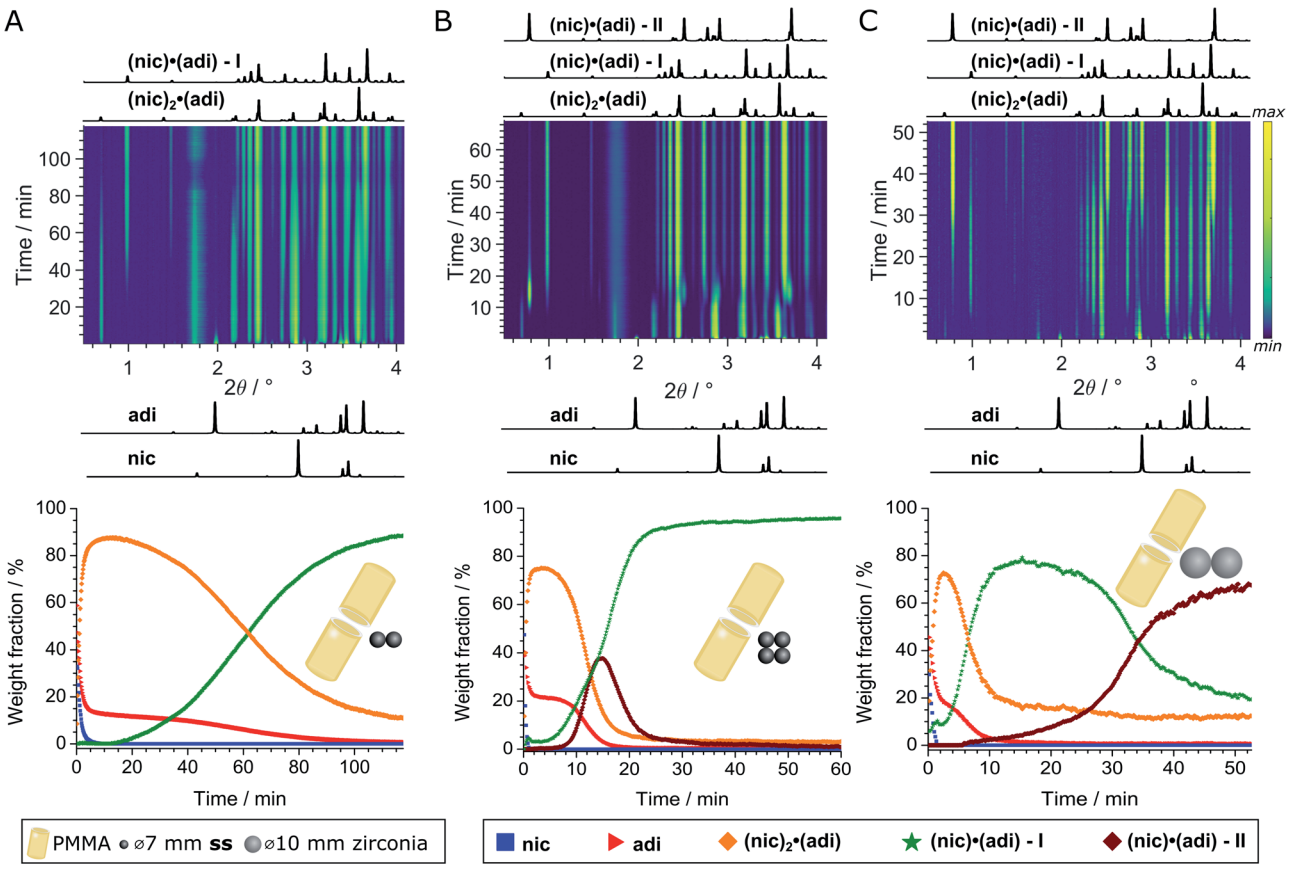

Fig. 4 Top: *In situ* monitoring of the LAG reaction with ACN ($\eta = 0.125$ μL mg^{-1}) with bottom the corresponding reaction profiles derived from quantitative phase *via* sequential Rietveld refinement for the reaction using (A) two 1.4 g **ss**, (B) four 1.4 g **ss**, and (C) two 2.9 g zirconia balls. Calculated XRPD patterns ($\lambda = 0.207$ Å) of reactants and cocrystals are shown below and above the 2D plots. The weight fractions of **nic** (blue squares), **adi** (red triangles), **(nic)$_2$·(adi)** (orange diamond), **(nic)·(adi)** – I (green star), and **(nic)·(adi)** – II (burgundy diamond) are colored identical in (A)-(C). The weight fraction of **(nic)$_2$·(adi)** cocrystal is intrinsically overestimated in (A and C), see ESI.‡

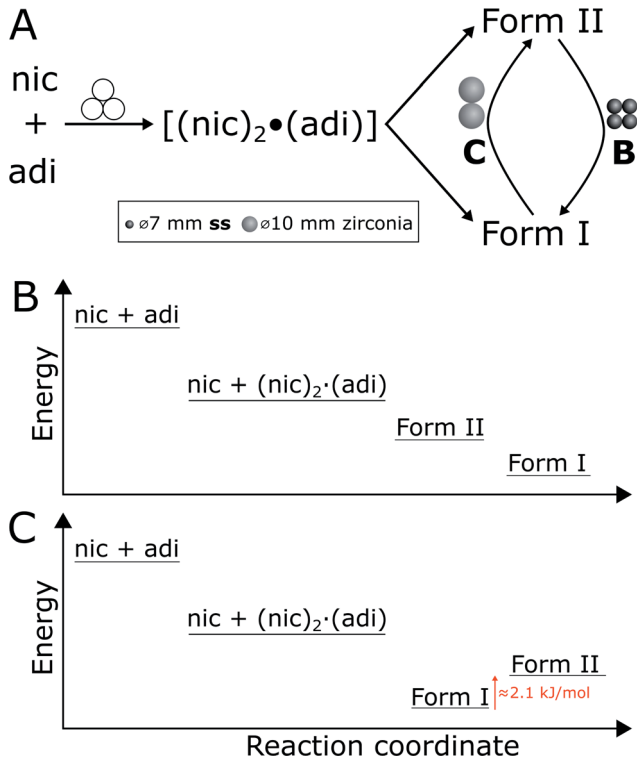

Fig. 5 (A) Reaction scheme for *in situ* monitoring reactions in experiments B and C, using a total weight of milling media of 5.6 and 5.8 g, respectively. Reaction using four **ss** balls led to Form I, while two zirconia balls let to Form II as final product. (B and C) Schematic representation of the energy diagram for the *in situ* monitoring reactions in experiments B using **ss** and (C) using zirconia balls in PMMA jars, as reaction progresses. The enthalpy difference of 2.1 kJ mol^{-1} (at transition temperature) between Forms I and II is based on the DSC measurements.

of **(nic)$_2$·(adi)** being complete after *ca.* 2.5 minutes. While both Form I and II **(nic)·(adi)** again appeared concomitantly, under these conditions the growth of Form I was significantly faster than for Form II. As a result, after 15 minutes the reaction mixture was composed mostly of Form I **(nic)·(adi)**. Further milling leads to the process opposite to that seen in experiment B, *i.e.* direct conversion of Form I into Form II. Considering that Form I is the thermodynamically more stable form of the **(nic)·(adi)** cocrystal until the transition point temperature measured to be *ca.* 85–90 °C, these observations that the mechanochemical formation of the metastable polymorph (Form II) proceeds *via* the thermodynamically more stable phase (Form I) are in contrast to Ostwald's rule of stages (Fig. 5B).

Experimental and theoretical evaluation of polymorph stability

The thermodynamic relationship between two **(nic)·(adi)** polymorphs was investigated experimentally and by theoretical periodic density functional theory (DFT) calculations. Experimental studies were conducted by solvent-mediated phase transformation[40] in a static system, in a slurry, by long-term stability measurements, and by thermal analysis. Solvent-mediated experiments under static conditions, starting with a physical mixture of both polymorphs, led to the disappearance of Form II (Fig. S4‡) with Form I remaining as the main crystalline phase. Slurry experiments were more difficult to interpret since, independent of the starting composition, some of the mixtures eventually transformed into **(nic)$_2$·(adi)** with release of pure **adi** (Fig. S5‡). Several long-term stability measurements revealed on one hand a slow transformation of Form II into Form I over a couple of months in air at room temperature, as evidenced by the appearance of Bragg reflections of Form I in a previously phase-pure sample of Form II (Fig. 6A and S6‡). On the other hand, complete transformation of a reaction mixture of **(nic)$_2$·(adi)**, **(nic)·(adi)** Form I and Form II, as well as **adi** into Form I was observed within 7 months upon storage (Fig. 6A and S6‡). These results are consistent with Form I being the thermodynamically preferred one in this system. Thermal behavior of both polymorphs was investigated in detail by thermal analysis and variable temperature XRPD (VT-XRPD) measurements. A combined differential scanning calorimetry and thermogravimetric analysis (DSC-TGA) of Form II showed a sharp endothermic signal with an onset at *ca.* 124 °C upon heating, corresponding to melting. Crystallisation upon cooling took place at *ca.* 100 °C, without any notable changes in sample weight throughout the experiment (Fig. S10‡). In contrast, two distinct endothermic signals appeared in the DSC thermograms of Form I upon heating, starting at *ca.* 84 °C and 124 °C, again with no change in sample weight (Fig. 6B, S9 and S11–S13‡). The first signal was attributed to the transformation of Form I into Form II, as confirmed by VT-XRPD measurements which revealed a transition taking place in the range 85–100 °C (Fig. 6C and S7‡). The second DSC signal is assigned to melting of Form II, with crystallisation occurring upon cooling at *ca.* 106 °C (Fig. S9‡). No transformation of Form II into Form I was observed by VT-XRPD experiments upon cooling to −180 °C (Fig. S8‡). The crystallographic calculated density of Form II is somewhat lower (1.32 g cm^{-3}) compared to Form I (1.36 g cm^{-3}). In conclusion, Form I is the thermodynamically more stable form at ambient condition, with Form II as the enantiotropically-related high temperature polymorph. This is in excellent agreement with crystallographic calculated densities, different long-term stability, as well as VT-XRPD, and thermal measurements.

The transition enthalpy for the polymorphic transformation of Form I into Form II was calculated based on the integrated area of the endothermic signal in DSC measurements (see ESI‡). The enthalpy for the transformation of Form I to Form II is *ca.* 1.6(2) kJ mol^{-1} at the transition temperature (*ca.* 90 °C), which translates to 2.1(3) kJ mol^{-1} at the temperature of mechanochemical milling (estimated to be *ca.* 35 °C), based on the molar heat capacity of Form I evaluated from DSC measurements (see ESI, Tables S2–S4, Fig. S10, and S11–S13‡).

The relative stability of **(nic)·(adi)** polymorphs was also explored by periodic DFT calculations, using the plane-wave DFT code CASTEP.[41] Crystal structures of all the cocrystals as well as **nic** and **adi** reactants were geometry-optimised using the Perdew–Burke–Ernzerhof (PBE)[42] functional combined with

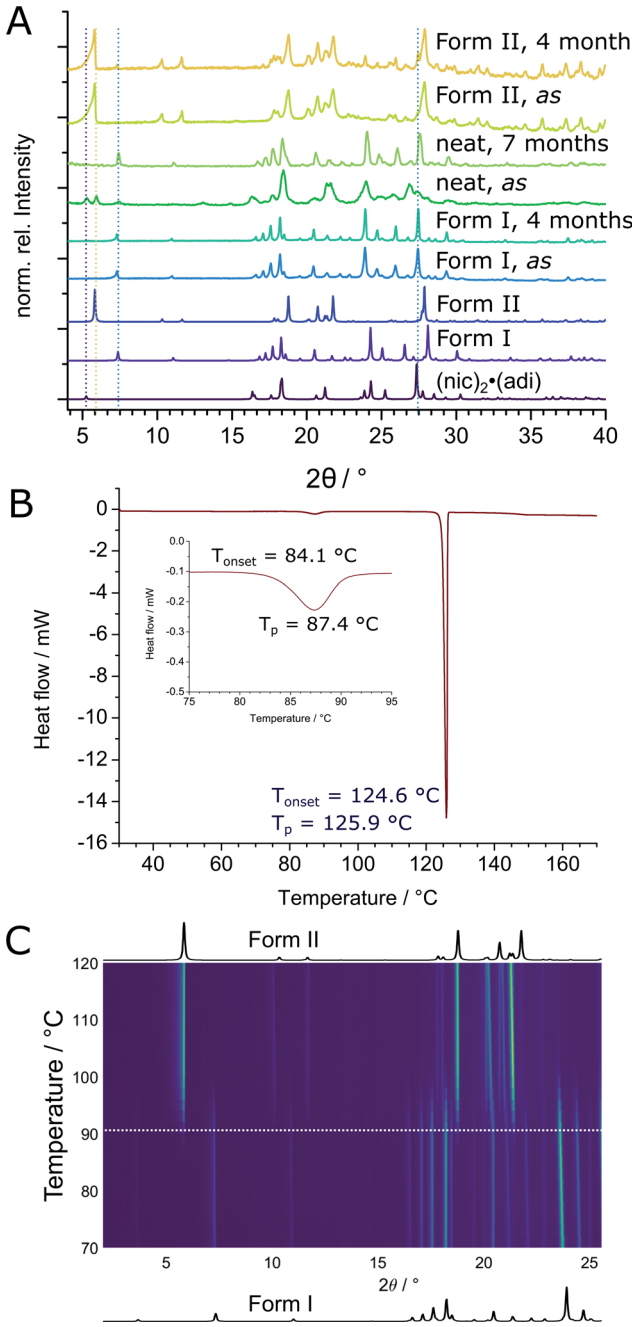

Fig. 6 (A) Comparison of measured and calculated XRPD patterns for the different long-term stability measurements. From bottom to top: calculated XRPD patterns of **(nic)$_2$·(adi)**, **(nic)·(adi)** – Form I, and Form II. Measured XRPD patterns of as synthesized Form I and after 4 months, as synthesized (*as*) reaction mixture after neat grinding for 60 min and after 7 months, as synthesized Form II and after 4 months (B) DSC measurement of Form I with the onset of polymorphic transition into Form II at 84.1 °C and melting of Form II at *ca.* 124.6 °C (ΔT = 1 °C min^{-1}). (C) High temperature XRPD measurement of Form I with calculated XRPD patterns of **(nic)·(adi)** Form I and II below and above the 2D plot, respectively.

many-body dispersion (MBD*)[43–45] correction scheme. In these calculations, the geometries of observed phases, *i.e.* atomic coordinates and lattice parameters, were fully optimised to yield the total electronic energies. The calculated energy of **(nic)$_2$·(adi)** cocrystal with respect to the starting reactant mixture for a 1 : 1 reaction was −8.5 kJ mol^{-1}. The corresponding relative energies for **(nic)·(adi)** Form I and **(nic)·(adi)** Form II were −7.5 kJ mol^{-1} and −10.2 kJ mol^{-1}, respectively (Table S5‡). While calculations indicate that cocrystallisation of **nic** and **adi** is thermodynamically favourable, the calculated energies for all three cocrystals differ by less than 3 kJ mol^{-1}, which is comparable to the experimentally determined transition enthalpy. This, however, also means that the relative energy ranking of the three cocrystals cannot be reliably established by herein explored periodic DFT calculations.[46,47]

Discussion

The described milling experiments demonstrate that the course and polymorphic outcome of mechanochemical cocrystallisation can strongly be affected by choice of material from which the milling media or the entire milling assembly are made. Whereas mechanochemical reactions of metal–organic materials were recently shown to follow Ostwald's rule of stages,[23a] the herein explored cocrystal of **nic** and **adi** exhibits significantly different behavior. In particular, our study shows that either the high temperature Form II or the room temperature Form I of the **(nic)·(adi)** cocrystal is obtained, depending on choice of milling assembly. While the observed appearance of Form II as an intermediate in the mechanochemical formation of the more stable Form I is not surprising (Fig. 4 and 5B), the ability to also obtain Form II as the final product, *via* the thermodynamically more stable Form I as an intermediate, is in clear contrast with Ostwald's rule of stages (Fig. 5C). Moreover, our study shows that the two forms can even readily interconvert depending on the choice of milling assembly, *i.e.* milling jars and balls.

We tentatively explain such behavior, unprecedented in mechanochemical cocrystallisation, by the small energy difference between the two cocrystal polymorphs. Specifically, we propose that the difference in stability of Forms I and II is sufficiently small that minor changes in the mechanical energy input during milling can lead to preferred formation of either one or the other polymorph. This scenario is somewhat reminiscent of the proposal made over 120 years ago by M. Carey Lea, the "father of mechanochemistry", who suggested that mechanochemical reactions can enable the formation of metastable products in systems that "…possessed an equilibrium so singularly balanced as to be affected by the slightest action…".[48] The herein presented system belongs to this category, with a ΔH between Forms I and II of only 2.1(3) kJ mol^{-1} (at the transition temperature, *ca.* 90 °C). We propose that the observed selectivity for either Form I or Form II is related to a difference in the efficiency of transfer of mechanical energy from the milling assembly to the sample (Fig. 5A). Specifically, formation of Form II, and transformation of Form I to Form II, was achieved by milling in **ss** jars, while the opposite processes were observed upon milling in PMMA jars. As the jar volume,¶ sample amount and choice of milling media were identical in those experiments, we relate the difference in reaction outcome to a more efficient transfer of mechanical energy using a **ss** jar

of higher elastic properties compared to PMMA, evidenced by respective Young's moduli of 208 GPa [49] (for 440C **ss** jar material) to *ca.* 3–5 GPa.[50]

The importance of energy input in order to overcome the energy threshold for the formation of Form II is also evidenced by *in situ* monitoring studies, which were all conducted in PMMA jars of identical volume and weight. In this case, the appearance of Form II was first induced by increasing the number of **ss** media and their overall weight. Previous studies indicate that such changes result in a higher energy input in a mechanochemical reaction and, under these conditions, Form II was as observed as a metastable, short-lived intermediate consistent with Ostwald's rule of stages. However, more efficient energy transfer has also enabled the formation of Form II as the final reaction product in PMMA jars. This was observed by switching from **ss** media to those based on the more elastic material zirconia, with Young's modulus ~221–223 GPa.[51] By replacing four **ss** (total weight 5.6 grams) balls with two zirconia balls (total weight 5.8 grams), it was possible to conduct the experiment with almost identical weight of milling media. As there was no significant change in overall sample weight or choice of milling jars between these experiments, the observed difference in reactivity can be related to more efficient energy transfer due to choice of material. It is, however, important to note that energy input could also be affected by differences in motion and impact of individual balls.[26b,27b]

While we cannot fully exclude the importance of changes in additional factors such as particle size,[52] frictional properties of the mixture, and/or temperature, we are confident that the observed results are not associated to seeding and surface templating effects, as the same set of PMMA jars was used for the mechanosynthesis of both polymorphs. Previous studies of mechanochemical organic reactions have indicated that the choice of milling media and/or jars can have a significant impact on temperature and frictional properties of the milled reaction mixture.[25,30,33b] We attempted to measure the temperature of reaction mixture using an infrared probe immediately after milling, but did not observe any significant differences between reactions in PMMA or **ss** jars. Indeed, the evolution of temperature in a mechanochemical reaction is difficult to establish with certainty,[53] and surface temperature measurements are not expected to be highly reliable, as Kubota *et al.* have shown that the temperature can vary significantly (*ca.* 10 °C) across the jar surface.[54]

Conclusions

In conclusion, we have demonstrated that the formation and interconversion of polymorphs during mechanochemical cocrystallisation is strongly affected, and can be controlled, by the choice of milling assembly. While milling reactions have previously been shown to follow the Ostwald's rule of stages,[23a] our results demonstrate that exceptions can be observed for systems in which different products exhibit only a small difference in energy. This is the case for the herein described polymorphs of the cocrystal of nicotinamide and adipic acid, exhibiting a ~2 kJ mol^{-1} difference in stability, whose selective formation can be accomplished by changes to the milling assembly leading to different energy inputs. While this represents the first experimental report of polymorphs that can mechanochemically interconvert by modification of the milling assembly, similar behaviour might be observable for other enantiotropically related polymorphic systems that are sufficiently close in energy.[55] Moreover, while previous work focused solely on the choice and amount of liquid additive to control and explore polymorphism in mechanochemical cocrystallisation, our work shows that the choice of milling assembly itself can also play a crucial role in mechanochemical polymorph selection and, indeed, be used to interconvert between cocrystal polymorphs.

To the best of our knowledge, this work represents the first demonstration of how a mechanochemical reaction can be directed to produce either thermodynamically stable or metastable cocrystal polymorphs, only by changes to the milling jar and/or balls. We believe that further studies of how the choice of milling assembly affects product polymorphism might provide a means to design more reliable mechanochemical synthesis procedures and avoid potential obstacles in mechanochemical solid form development, such as the recently discussed "disappearing polymorph"[56,57] or "hidden cocrystal"[58] phenomena.

Conflicts of interest

There are no conflicts to declare.

Acknowledgements

We thank Drs Sandra Kaabel and Dritan Hasa for valuable scientific discussions. Dr Robin S. Stein is acknowledged for collecting ssNMR spectra and scientific discussions. We thank Dr Hatem M. Titi for help with DSC measurements. L. S. G acknowledges financial support from the Swiss National Science Foundation (Grant P2SKP2_187638). M. A. acknowledges the financial support of the National Science Center of Poland (Grant 2018/31/D/ST5/03619). T. F. acknowledges the financial support of the NSERC Discovery Grant (RGPIN-2017-06467), NSERC Discovery Accelerator award (RGPAS 507837-17), and the NSERC E. W. R. Steacie Memorial Fellowship (SMFSU 507347-17). This article is based upon work from COST Action CA18112 (https://www.mechsustind.eu) supported by COST (European Cooperation in Science and Technology, https://www.cost.eu). This research was enabled in part by support provided by Calcul Québec (https://www.calculquebec.ca) and Compute Canada (https://www.computecanada.ca).

Notes and references

§ Reactions by neat milling are generally expected to be slower compared to LAG reactions, see for example: N. Shan, F. Toda and W. Jones, *Chem. Commun.*, 2002, 2372–2373.

¶ Whereas the jar volume was different during synthesis for PMMA (15 mL) and **ss** jars (Retsch, 10 mL), it was identical for the interconversion reaction using 15 mL **ss** jars, see ESI.‡

1 (*a*) T. Friščić, C. Mottillo and H. M. Titi, *Angew. Chem., Int. Ed.*, 2020, **59**, 1018–1029; (*b*) E. Colacino, A. Porcheddu, C. Charnay and F. Delogu, *React. Chem. Eng.*, 2019, **4**, 1179–1188; (*c*) W. Pickhardt, S. Grätz and L. Borchardt, *Chem.–Eur. J.*, 2020, DOI: 10.1002/chem.202001177; (*d*) G.-W. Wang, *Chem. Soc. Rev.*, 2013, **42**, 7668–7700; (*e*) J. L Howard, Q. Cao and D. L. Browne, *Chem. Sci.*, 2018, **9**, 3080–3094.

2 (*a*) S. L. James, C. J. Adams, C. Bolm, D. Braga, P. Collier, T. Friščić, F. Grepioni, K. D. M. Harris, G. Hyett, W. Jones, A. Krebs, J. Mack, L. Maini, A. G. Orpen, I. P. Parkin, W. C. Shearouse, J. W. Steed and D. C. Waddell, *Chem. Soc. Rev.*, 2011, **41**, 413–447; (*b*) T. K. Achar, A. Bose and P. Mal, *Beilstein J. Org. Chem.*, 2017, **13**, 1907–1931; (*c*) J. G. Hernández and C. Bolm, *J. Org. Chem.*, 2017, **82**, 4007–4019; (*d*) E. Colacino, G. Dayaker, A. Morere and T. Friščić, *J. Chem. Educ.*, 2019, **96**, 766–771; (*e*) L. Konnert, F. Lamaty, J. Martinez and E. Colacino, *Chem. Rev.*, 2017, **117**, 13757–13809; (*f*) K. Kubota, Y. Pang, A. Miura and H. Ito, *Science*, 2019, **366**, 1500–1504.

3 B. P. Biswal, S. Chandra, S. Kandambeth, B. Lukose, T. Heine and R. Banerjee, *J. Am. Chem. Soc.*, 2013, **135**, 5328–5331.

4 S. Chandra, S. Kandambeth, B. P. Biswal, B. Lukose, S. M. Kunjir, M. Chaudhary, R. Babarao, T. Heine and R. Banerjee, *J. Am. Chem. Soc.*, 2013, **135**, 17853–17861.

5 (*a*) A. D. Katsenis, A. Puškarić, V. Štrukil, C. Mottillo, P. A. Julien, K. Užarević, M.-H. Pham, T.-O. Do, S. A. J. Kimber, P. Lazić, O. Magdysyuk, R. E. Dinnebier, I. Halasz and T. Friščić, *Nat. Commun.*, 2015, **6**, 6662; (*b*) D. Prochowicz, J. Nawrocki, M. Terlecki, W. Marynowski and J. Lewiński, *Inorg. Chem.*, 2018, **57**, 13437–13442.

6 C. Cappuccino, F. Farinella, D. Braga and L. Maini, *Cryst. Growth Des.*, 2019, **19**, 4395–4403.

7 (*a*) P. Baláž, M. Achimovičová, M. Baláž, P. Billik, Z. Cherkezova-Zheleva, J. M. Criado, F. Delogu, E. Dutková, E. Gaffet, F. J. Gotor, R. Kumar, I. Mitov, T. Rojac, M. Senna, A. Streletskii and K. Wieczorek-Ciurowa, *Chem. Soc. Rev.*, 2013, **42**, 7571–7637; (*b*) H. Schreyer, R. Eckert, S. Immohr, J. de Bellis, M. Feldehoff and F. Schüth, *Angew. Chem., Int. Ed.*, 2019, **58**, 11262–11265.

8 M. Leonardi, M. Villacampa and J. C. Menéndez, *Chem. Sci.*, 2018, **9**, 2042–2064.

9 G.-W. Wang, *Chem. Soc. Rev.*, 2013, **42**, 7668–7700.

10 A. Bruckmann, A. Krebs and C. Bolm, *Green Chem.*, 2008, **10**, 1131–1141.

11 (*a*) D. Hasa and W. Jones, *Adv. Drug Delivery Rev.*, 2017, **117**, 147–161; (*b*) D. Braga, L. Maini and F. Grepioni, *Chem. Soc. Rev.*, 2013, **42**, 7638–7648; (*c*) D.-K. Bučar, S. Filip, M. Arhangelskis, G. O Lloyd and W. Jones, *CrystEngComm*, 2013, **15**, 6289–6291.

12 (*a*) S. A. Ross, D. A. Lamprou and D. Douroumis, *Chem. Commun.*, 2016, **52**, 8772–8786; (*b*) S. Lukin, I. Lončarić, M. Tireli, T. Stolar, M. V. Blanco, P. Lazić, K. Užarević and I. Halasz, *Cryst. Growth Des.*, 2018, **18**, 1539–1547.

13 I. R. Speight, I. Huskić, M. Arhangelskis, H. M. Titi, R. S. Stein, T. P. Hanusa and T. Friščić, *Chem.–Eur. J.*, 2020, **26**, 1811–1818.

14 T. Friščić, S. L. Childs, S. A. A. Rizvi and W. Jones, *CrystEngComm*, 2009, **11**, 418–426.

15 D. Hasa, G. Schneider Rauber, D. Voinovich and W. Jones, *Angew. Chem., Int. Ed.*, 2015, **54**, 7371–7375.

16 D. Hasa, E. Miniussi and W. Jones, *Cryst. Growth Des.*, 2016, **16**, 4582–4588.

17 T. Friščić and W. Jones, *Cryst. Growth Des.*, 2009, **9**, 1621–1637.

18 A. V. Trask, W. D. S. Motherwell and W. Jones, *Chem. Commun.*, 2004, 890–891.

19 A. V. Trask, N. Shan, W. D. S. Motherwell, W. Jones, S. Feng, R. B. H. Tan and K. J. Carpenter, *Chem. Commun.*, 2005, 880–882.

20 P. A. Julien, K. Užarević, A. D. Katsenis, S. A. J. Kimber, T. Wang, O. K. Farha, Y. Zhang, J. Casaban, L. S. Germann, M. Etter, R. E. Dinnebier, S. L. James, I. Halasz and T. Friščić, *J. Am. Chem. Soc.*, 2016, **138**, 2929–2932.

21 I. Halasz, A. Puškarić, S. A. J. Kimber, P. J. Beldon, A. M. Belenguer, F. Adams, V. Honkimäki, R. E. Dinnebier, B. Patel, W. Jones, V. Štrukil and T. Friščić, *Angew. Chem., Int. Ed.*, 2013, **52**, 11538–11541.

22 S. H. Lapidus, A. Naik, A. Wixtrom, N. E. Massa, V. Ta Phuoc, L. del Campo, S. Lebègue, J. G. Ángyán, T. Abdel-Fattah and S. Pagola, *Cryst. Growth Des.*, 2014, **14**, 91–100.

23 (*a*) Z. Akimbekov, A. D. Katsenis, G. P. Nagabhushana, G. Ayoub, M. Arhangelskis, A. J. Morris, T. Friščić and A. Navrotsky, *J. Am. Chem. Soc.*, 2017, **139**, 7952–7957; (*b*) M. Arhangelskis, A. D. Katsenis, N. Novendra, Z. Akimbekov, D. Gandrath, J. M. Marrett, G. Ayoub, A. J. Morris, O. K. Farha, T. Friščić and A. Navrotsky, *Chem. Mater.*, 2019, **31**, 3777–3783; (*c*) J. C. Burley, M. J. Duer, R. S. Stein and R. M. Vrcelj, *Eur. J. Pharm. Sci.*, 2007, **31**, 271–276; (*d*) M. Arhangelskis, F. Topić, P. Hindle, R. Tran, A. J. Morris, D. Cinčić and T. Friščić, *Chem. Commun.*, 2020, **56**, 8293–8296.

24 P. A. Julien, I. Malvestiti and T. Friščić, *Beilstein J. Org. Chem.*, 2017, **13**, 2160–2168.

25 X. Ma, W. Yuan, S. E. J. Bell and S. L. James, *Chem. Commun.*, 2014, **50**, 1585–1587.

26 (*a*) R. Schmidt, H. M. Scholze and A. Stolle, *Int. J. Ind. Chem.*, 2016, **7**, 181–186; (*b*) R. Schmidt, C. F. Burmeister, M. Baláž, A. Kwade and A. Stolle, *Org. Process Res. Dev.*, 2015, **19**, 427–436; (*c*) A. Stolle, R. Schmidt and K. Jacob, *Faraday Discuss.*, 2014, **170**, 267–286.

27 (*a*) H. Kulla, F. Fischer, S. Benemann, K. Rademann and F. Emmerling, *CrystEngComm*, 2017, **19**, 3902–3907; (*b*) F. Fischer, N. Fendel, S. Greiser, K. Rademann and F. Emmerling, *Org. Process Res. Dev.*, 2017, **21**, 655–659.

28 Mechanochemical cocrystallization of caffeine and trifluoroacetic acid can lead to different polymorphic outcomes, depending on the total amount of material in the jar, and independent of reaction time: A. V. Trask, J. van de Streek, W. D. S. Motherwell and W. Jones, *Cryst. Growth Des.*, 2005, **5**, 2233–2241.

29 N. R. Rightmire and T. P. Hanusa, *Dalton Trans.*, 2016, **45**, 2352–2362.

30 A. A. L. Michalchuk, I. A. Tumanov and E. V. Boldyreva, *J. Mater. Sci.*, 2018, **53**, 13380–13389.
31 K. S. McKissic, J. T. Caruso, R. G. Blair and J. Mack, *Green Chem.*, 2014, **16**, 1628–1632.
32 A. A. L. Michalchuk, I. A. Tumanov and E. V. Boldyreva, *CrystEngComm*, 2019, **21**, 2174–2179.
33 (*a*) M. Carta, S. L. James and F. Delogu, *Molecules*, 2019, **24**, 3600–3613; (*b*) I. A. Tumanov, A. F. Achkasov, E. V. Boldyreva and V. V. Boldyrev, *CrystEngComm*, 2011, **13**, 2213–2216.
34 (*a*) J. Andersen and J. Mack, *Angew. Chem., Int. Ed.*, 2018, **57**, 13062–13065; (*b*) J. M. Andersen and J. Mack, *Chem. Sci.*, 2017, **8**, 5447–5453.
35 M. Broseghini, M. D'Incau, L. Gelisio, N. M. Pugno and P. Scardi, *Materials & Design*, 2016, **110**, 365–374.
36 L. Takacs and V. Šepelák, *J. Mater. Sci.*, 2004, **39**, 5487–5489.
37 Kulla *et al.* recently reported the increased polymorphic stability of dimorphic cocrystals based on the used jar material, see: H. Kulla, C. Becker, A. A. L. Michalchuk, K. Linberg, B. Paulus and F. Emmerling, *Cryst. Growth Des.*, 2019, **19**, 7271–7279.
38 S. Karki, T. Friščić and W. Jones, *CrystEngComm*, 2009, **11**, 470–481.
39 (*a*) T. Friščić, I. Halasz, P. J. Beldon, A. M. Belenguer, F. Adams, S. A. J. Kimber, V. Honkimäki and R. E. Dinnebier, *Nat. Chem.*, 2013, **5**, 66–73; (*b*) I. Halasz, S. A. J. Kimber, P. J. Beldon, A. M. Belenguer, F. Adams, V. Honkimäki, R. C. Nightingale, R. E. Dinnebier and T. Friščić, *Nat. Protoc.*, 2013, **8**, 1718–1729.
40 G. G. Z. Zhang, R. F. Henry, T. B. Borchardt and X. Lou, *J. Pharm. Sci.*, 2007, **96**, 990–995.
41 S. J. Clark, M. D. Segall, C. J. Pickard, P. J. Hasnip, M. I. J. Probert, K. Refson and M. C. Payne, *Z. Kristallogr. - Cryst. Mater.*, 2005, **220**, 567–570.
42 J. P. Perdew, K. Burke and M. Ernzerhof, *Phys. Rev. Lett.*, 1996, **77**, 3865–3868.
43 A. M. Reilly and A. Tkatchenko, *Chem. Sci.*, 2015, **6**, 3289–3301.
44 A. Ambrosetti, A. M. Reilly, R. A. DiStasio and A. Tkatchenko, *J. Chem. Phys.*, 2014, **140**, 18A508.
45 A. Tkatchenko, R. A. DiStasio, R. Car and M. Scheffler, *Phys. Rev. Lett.*, 2012, **108**, 236402.
46 C. R. Taylor and G. M. Day, *Cryst. Growth Des.*, 2018, **18**, 892–904.
47 E. Schur, J. Bernstein, L. S. Price, R. Guo, S. L. Price, S. H. Lapidus and P. W. Stephens, *Cryst. Growth Des.*, 2019, **19**, 4884–4893.
48 M. C. Lea, *Am. J. Sci.*, 1892, **34**, 527–531.
49 H. M. Ledbetter, N. V. Frederick and M. W. Austin, *J. Appl. Phys.*, 1980, **51**, 305–309.
50 (*a*) G. Wei and B. Bhushan, *J. Vac. Sci. Technol.*, 2005, **A23**, 811–819; (*b*) C. Ishiyama and Y. Higo, *J. Polym. Sci., Part B: Polym. Phys.*, 2002, **40**, 460–465.
51 J. W. Adams, R. Ruh and K. S. Mazdiyasni, *J. Am. Ceram. Soc.*, 1997, **80**(4), 903–908.
52 A. M. Belenguer, G. I. Lampronti, A. J. Cruz-Cabeza, C. A. Hunter and J. K. M. Sanders, *Chem. Sci.*, 2016, **7**, 6617–6627.
53 K. Užarević, N. Ferdelji, T. Mrla, P. A. Julien, B. Halasz, T. Friščić and I. Halasz, *Chem. Sci.*, 2018, **9**, 2525–2532.
54 K. Kubota, Y. Pang, A. Miura and H. Ito, *Science*, 2019, **366**, 1500–1504.
55 (*a*) J. Nyman and G. M. Day, *CrystEngComm*, 2015, **17**, 5154–5165; (*b*) R. M. Bhardwaj, J. A. McMahon, J. Nyman, L. S. Price, S. Konar, I. D. H. Oswald, C. R. Pulham, S. L. Price and S. M. Reutzel-Edens, *J. Am. Chem. Soc.*, 2019, **141**, 13887–13897.
56 J. D. Dunitz and J. Bernstein, *Acc. Chem. Res.*, 1995, **28**, 193–200.
57 D. Hasa, M. Marosa, D.-K. Bučar, M. K. Corpinot, D. Amin, B. Patel and W. Jones, *Cryst. Growth Des.*, 2020, **20**, 1119–1129.
58 D.-K. Bučar, G. M. Day, I. Halasz, G. G. Z. Zhang, J. R. G. Sander, D. G. Reid, L. R. MacGillivray, M. J. Duer and W. Jones, *Chem. Sci.*, 2013, **4**, 4417–4425.

